

# Recruitment of Donor T Cells to the Eyes During Ocular GVHD in Recipients of MHC-Matched Allogeneic Hematopoietic Stem Cell Transplants

Samantha Herretes,<sup>1</sup> Duncan B. Ross,<sup>2</sup> Stephanie Duffort,<sup>1</sup> Henry Barreras,<sup>2</sup> Tan Yaohong,<sup>1</sup> Ali M. Saeed,<sup>1</sup> Juan C. Murillo,<sup>1</sup> Krishna V. Komanduri,<sup>3,4</sup> Robert B. Levy,<sup>1,2,4</sup> and Victor L. Perez<sup>1,2,4</sup>

<sup>1</sup>Department of Ophthalmology, University of Miami Miller School of Medicine, Miami, Florida, United States

<sup>2</sup>Department of Microbiology and Immunology, University of Miami Miller School of Medicine Sylvester Comprehensive Cancer Center, Miami, Florida, United States

<sup>3</sup>Adult Stem Cell Transplant Program, University of Miami Miller School of Medicine Sylvester Comprehensive Cancer Center, Miami, Florida, United States

<sup>4</sup>Department of Medicine, University of Miami Miller School of Medicine Sylvester Comprehensive Cancer Center, Miami, Florida, United States

Correspondence: Victor L. Perez; vperez4@med.miami.edu.

Submitted: September 7, 2014

Accepted: January 13, 2015

Citation: Herretes S, Ross DB, Duffort S, et al. Recruitment of donor T cells to the eyes during ocular GVHD in recipients of MHC-matched allogeneic hematopoietic stem cell transplants. *Invest Ophthalmol Vis Sci*.

2015;56:2348–2357. DOI:10.1167/iops.1415630

**PURPOSE.** The primary objective of the present study was to identify the kinetics and origin of ocular infiltrating T cells in a preclinical model of graft-versus-host disease (GVHD) that induces eye tissue damage.

**METHODS.** Graft-versus-host disease was induced using an major histocompatibility complex (MHC)-matched, minor histocompatibility-mismatched hematopoietic stem cell transplant (HSCT) model. This approach, which utilized congenic and EGFP-labeled donor populations, mimics a matched, clinically unrelated donor (MUD) cell transplant. Systemic and ocular GVHD were assessed at varying time points using clinical examination, intravital microscopy, immune phenotype via flow cytometric analyses, and immunohistochemical staining.

**RESULTS.** Following transplant, we observed characteristic changes in GVHD-associated immune phenotype as well as clinical signs present in recipients post transplant. Notably, the kinetics of the systemic changes and the ocular damage paralleled what is observed clinically, including damage to the cornea as well as the conjunctiva and lacrimal gland. Importantly, the infiltrate contained predominantly donor CD4 as well as CD8 T cells with an activated phenotype and macrophages together with effector cytokines consistent with the presence of a TH1 alloreactive population.

**CONCLUSIONS.** Overall, the findings here unequivocally demonstrated that donor T cells compose part of the corneal and ocular adnexa infiltrate in animals undergoing ocular GVHD. In total, the results describe a novel and promising preclinical model characterized by both systemic and ocular changes as detected in significant numbers of patients undergoing GVHD following allo-HSCT, which can help facilitate dissecting the underlying immune mechanisms leading to damage associated with ocular GVHD.

**Keywords:** ocular GVHD, T-cell infiltrates, allogeneic hematopoietic stem cell transplant

Allogeneic hematopoietic stem cell transplantation (HSCT) has become the standard of care for the treatment of several life-threatening hematologic malignancies as well as certain immunodeficiency diseases.<sup>1,2</sup> Unfortunately, as the survival rate of patients with these diseases is improved, the quality of life is negatively impacted by the development of graft-versus-host disease (GVHD). Graft-versus-host disease is a complex, multiorgan disorder arising from an immunologic attack by donor alloreactive T cells that result in damage to vital organs including the liver, skin, hematopoietic compartment, and the ocular surface of the eye.<sup>3–7</sup> Ocular GVHD occurs in >60% of these patients and is characterized by dry eye, conjunctiva damage, punctate keratopathy, corneal ulceration, and perforation.<sup>8–12</sup> Patients with ocular GVHD suffer and are incapacitated because of severe ocular discomfort, pain, and

poor vision.<sup>13,14</sup> Despite the high frequency of eye involvement in patients undergoing GVHD, little is known regarding the underlying immune mechanisms responsible for ocular GVHD, limiting the ophthalmic care of these patients to palliative therapies and global anti-inflammatory drugs.

Even though major advances have been made in the understanding of immune dysregulation in systemic GVHD, a critical question in the field is to understand the relationship between systemic and organ-specific GVHD. More specifically, a central unanswered question regarding systemic GVHD and subsequent damage in various tissues is the involvement of alloreactive and perhaps self-reactive responses, which have also been demonstrated post HSCT.<sup>15–20</sup> Systemic acute and chronic GVHD has been extensively studied with the use of a number of murine models differing in donor and recipient

strain combinations, genetic disparities, and conditioning regimens.<sup>21,22</sup> However, there are very few models that mimic the clinical ocular manifestations occurring, and most are associated with acute models of the disease.<sup>23,24</sup>

We wanted to identify a model in which ocular involvement is preceded by systemic GVHD to understand the immune mechanisms of ocular GVHD. Our group has developed a unique preclinical animal model in which lethally irradiated C3H.SW mice (H2<sup>b</sup>) infused with C57BL/6 (H2<sup>b</sup>) T cells + HSCT develop systemic and ocular GVHD with kinetics of onset similar to those observed in patients who develop eye complications with GVHD. The studies here demonstrate for the first time that ocular disease correlates with the presence of donor T cells in eye tissue and that this is also associated with the infiltration of macrophages (mΦ). In total, the present findings have identified alterations and pathology in the eye and adnexa reflective of ocular GVHD and unequivocally demonstrate the presence of donor T cells in the ocular surface.

## METHODS

### Animals

All animal studies were conducted according to protocols approved by the University of Miami Animal Care and Use Committee and in accordance with the ARVO Statement for the Use of Animals in Ophthalmic and Vision Research. C57BL/6J (B6) (H2<sup>b</sup>), C3H.SW (H2<sup>b</sup>), enhanced green fluorescent protein B6-EGFP transgenic (H2<sup>b</sup>), and B6-CXCR6<sup>-/-</sup>EGFP (Bonzo/STRL33) mice were obtained from Jackson Laboratory (Bar Harbor, ME, USA) and maintained in the animal facilities at the University of Miami School of Medicine. All mice used in experiments were 8 to 10 weeks old, free from ocular surface disease at baseline, and fed with a standard caloric diet for their age. The animals were routinely monitored prior to all procedures and until experiment end.

### Hematopoietic Stem Cell Transplantation

Mice (C3H.SW, H2<sup>b</sup>, Ly9.1<sup>+</sup>) were placed in a holding device to transport them for irradiation (total body irradiation 10.5 cGy using a Gamma Cell 40 [Company, City, State, Country] [35–40 rad/min] ~3 to 4 hours prior to transplantation) and provided antibiotic water (gentamycin, 25 mg/gallon) from day –3 to day 14 post transplant for prophylaxis against bacterial infection. In most experiments, the donor cells were obtained from unmanipulated mice of various genetic backgrounds. Donor B6 mice (H2<sup>b</sup>, Ly9.1<sup>-</sup>) were euthanized by cervical dislocation, and tissues were harvested and processed as previously described.<sup>25,26</sup> Femurs and tibiae were removed from donor mice and bone marrow cells (BMCs) flushed with cold RPMI-1640 using a syringe fitted with a 26-gauge needle. Donor marrow inoculum (TCD-BM) was prepared using anti-Thy-1.2 Miltenyi MACS (San Diego, CA, USA) magnetic beads and negative selection to remove T cells, washed, and adjusted before transplant to  $1 \times 10^7$ /mL. To prepare donor T cells, spleen and lymph node cells were incubated on anti-sIg-coated (Millipore, Darmstadt, Germany) plastic dishes for 45 minutes at 4°C to remove B cells. Nonadherent cells were harvested, and a small aliquot was stained with anti-CD4 and anti-CD8 mAb (BD Pharmingen, San Diego, CA, USA) to determine precise percentage contributions. Cell suspensions containing donor bone marrow and T cells were adjusted in serum-free RPMI to the desired concentration ( $4.6 \times 10^6$ /mL) for intravenous (0.5 mL) injection ( $2.3 \times 10^6$  T cells/mouse).

## Flow Cytometry

Lymph nodes, spleens, and peripheral blood were collected, and single-cell suspensions were prepared in PBS + 2% fetal calf serum + azide. Corneas were harvested, pooled, and incubated in  $1 \times$  PBS (pH 7.2–7.4) supplemented with EDTA (20 mM) for 15 minutes at 37°C. After washing, corneas were sliced into small fragments and incubated with collagenase (82 units/cornea; Sigma-Aldrich Corp., St. Louis, MO, USA) for 60 minutes at 37°C. Following the incubation, the corneas were dissociated into single-cell suspension and filtered using cell strainers (BD Falcon, Franklin Lakes, NJ, USA). After one wash with staining buffer ( $1 \times$  PBS supplemented with 1% FBS and 0.1% sodium azide (Sigma-Aldrich Corp.)), cells were stained for CD4, CD8, CD62L, and CD44 (eBiosciences, San Diego, CA, USA). Fluorescence-activated cell sorting (FACS) analysis of live lymphocytes was performed using Becton Dickinson LSRII and FACS Diva software (BD, San Jose, CA, USA) and FlowJo software (Tree Star, Ashland, OR, USA).

## Systemic and Ocular GVHD Assessment

Systemic GVHD was assessed using two analyses. Peripheral blood (and lymph node and spleen tissue in some experiments) was harvested to assess immune phenotype characteristic of GVHD using fluorescent conjugated mAbs to analyze CD4/CD8 ratio and B cell levels (anti-CD19 mAb). Animals were also monitored for clinical changes characteristic of GVHD. The onset/presence of GVHD was monitored before the HSCT and then weekly by a modified version of a standard scoring system previously described by Cooke et al.<sup>27</sup> This system incorporates seven clinical traits: weight loss, posture, activity, fur texture, skin integrity, alopecia, and presence of diarrhea. Each trait was scored from 0 to 2, with a range from 0 to 14.

Ocular GVHD was assessed using two analyses.

Corneal lysates were prepared as described above to assess immune phenotype characteristic of GVHD using mAbs to analyze CD4, CD8, CD62L, and CD44.

Clinical assessment was performed on all mice at baseline, and then weekly thereafter. Mice were anesthetized with isoflurane gas, and ocular surface was assessed using corneal fluorescein staining, performed by applying 3 μL of a 0.5% sodium fluorescein solution (Sigma-Aldrich Corp.) onto the eye. After washing with a balanced salt solution, the cornea was examined and photographed using an automated fluorescence microscope (Leica MZI6FA; Leica Microsystems, Wetzlar, Germany) and a cobalt blue light 2 to 3 minutes after fluorescein application. Punctate epithelial staining was scored using a previously described grading system in which the cornea is divided into five areas and a score is determined for each area, generating a clinical index with a maximum score of 15.<sup>28,29</sup>

## Histopathology and Immunohistochemistry

Mice were euthanized at 6 to 7 weeks after bone marrow transplantation. Eyes including the upper lids, conjunctiva, and fornix as well as lacrimal glands were harvested and embedded in OCT compound (Sakura Finetek USA, Inc., Torrance, CA, USA) and sectioned on a cryostat (Leica, Wetzlar, Germany) (–20°C) at 8 μm thick and collected on microscope slides. Histopathology was performed with hematoxylin/eosin (H&E) staining on corneal sections in order to evaluate parameters such as corneal thickness, inflammatory cell infiltration, vascularization, and integrity of the corneal endothelium. Lacrimal glands were stained with H&E, periodic acid Schiff (PAS), and Masson's trichrome. The counting of conjunctival goblet cells was performed as follows: 8-μm sections were obtained from the

TABLE. B6 Congenic and EGFP<sup>+</sup> Strains Used to Identify Donor T-Cell Origin

Donor BM	Donor T Cells	Recipient
1. B6 45.2 <sup>+</sup> /Ly9.1 <sup>-</sup> /CD90.2 <sup>+</sup>	B6-CD90.2 45.2 <sup>+</sup> /Ly9.1 <sup>-</sup> /CD90.2 <sup>+</sup>	C3H.SW 45.2 <sup>+</sup> /Ly9.1 <sup>+</sup> /CD90.2 <sup>+</sup>
2. B6-CD45.1 45.1 <sup>+</sup> /Ly9.1 <sup>-</sup> /CD90.2 <sup>+</sup>	B6-CD90.1 45.2 <sup>+</sup> /Ly9.1 <sup>-</sup> /CD90.1 <sup>+</sup>	C3H.SW 45.2 <sup>+</sup> /Ly9.1 <sup>+</sup> /CD90.2 <sup>+</sup>
3. B6-CD45.1 45.1 <sup>+</sup> /Ly9.1 <sup>-</sup> /CD90.2 <sup>+</sup>	B6-EGFP CD90.2 45.2 <sup>+</sup> /Ly9.1 <sup>-</sup> /CD90.2 <sup>+</sup>	C3H.SW 45.2 <sup>+</sup> /Ly9.1 <sup>+</sup> /CD90.2 <sup>+</sup>
4. B6-CD45.1 45.1 <sup>+</sup> /Ly9.1 <sup>-</sup> /CD90.2 <sup>+</sup>	B6-EGFP/CXCR6 45.2 <sup>+</sup> /Ly9.1 <sup>-</sup> /CD90.2 <sup>+</sup>	C3H.SW 45.2 <sup>+</sup> /Ly9.1 <sup>+</sup> /CD90.2 <sup>+</sup>

superior conjunctiva of all animals. They were initially formalin fixed on the slides and then stained with PAS. Goblet cell count was performed in at least 10 sections for each eye, and the average number was used for statistical analysis.

Immunohistochemistry was performed using the following protocol. The sections were fixed with 3% formaldehyde for 25 minutes, then pretreated with a blocking solution containing 0.05% Tween 20 and 3% BSA in PBS for 1 hour at room temperature to saturate nonspecific binding sites. The sections were then incubated 1 hour at room temperature with the primary antibody CD4, CD8 (T cells), CD11b (monocytes/macrophages), and Ly6G (neutrophils) from BD Pharmingen diluted 1/100 in PBS-Tween and 1% BSA. Sections were then rinsed for 10 minutes in PBS-Tween and incubated with 1:2000 goat anti-rat Alexa Fluor 594 (Invitrogen, Carlsbad, CA, USA) for 1 hour at room temperature. The sections were washed for 10 minutes in PBS Tween (3×) and 10 minutes in PBS (1×), coverslipped with Vectashield with

4',6-diamidino-2-phenylindole (DAPI; Vector Laboratory, Inc., Burlingame, CA, USA), and photographed in a Zeiss universal microscope (Carl Zeiss, Oberkochen, Germany) equipped for incident-light fluorescence.

### In Vivo Ocular Fluorescent Stereomicroscopy

Recipients of EGFP-labeled cell populations were evaluated at weekly time points using intravital fluorescent microscopy (Leica MZ16FA, EGFP 2 filter [excitation 480/40 nm, barrier 510 nm]), allowing measurement of EGFP expression in the cornea, which was quantified as mean green intensity (MGI) as described previously.<sup>30</sup> Photographs of the cornea were taken using the biomicroscope in a standardized fashion for all eyes. The image was analyzed using ImagePro software (Media Cybernetics, Rockville, MD, USA), and MGI was calculated for each cornea.

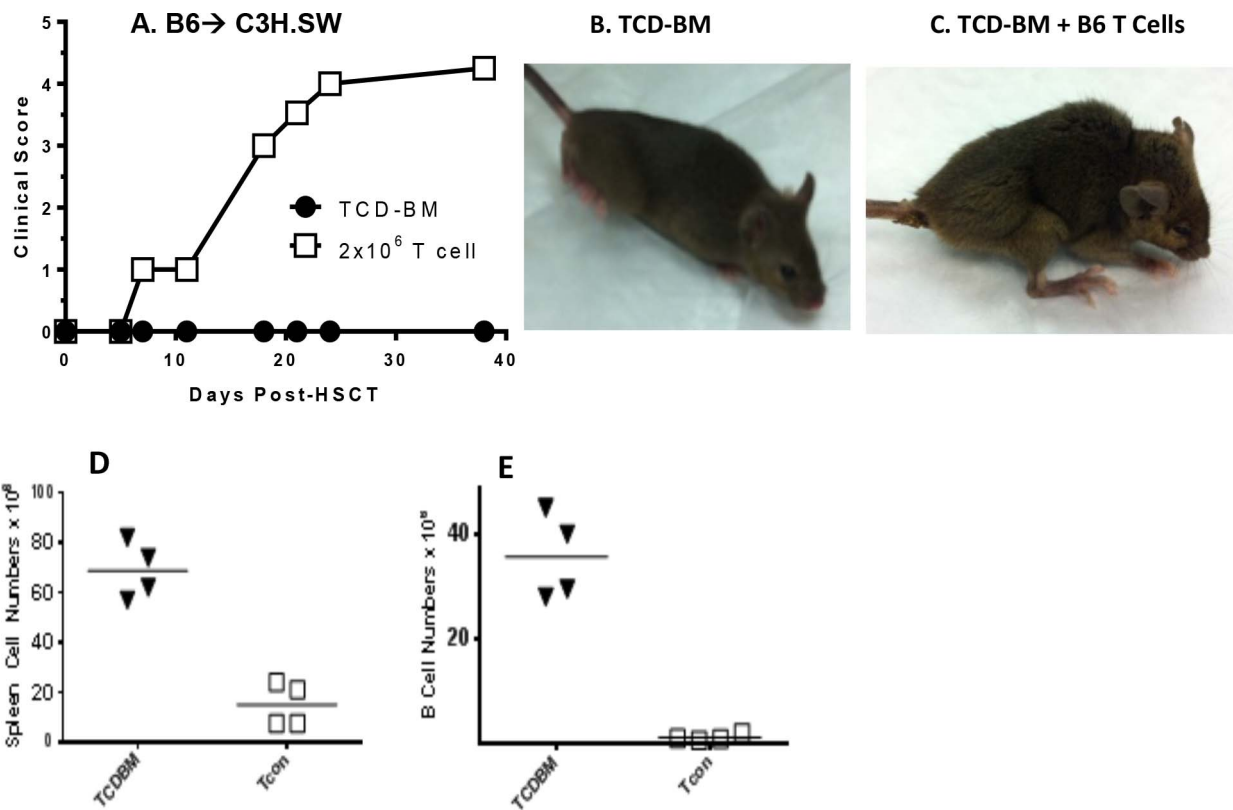
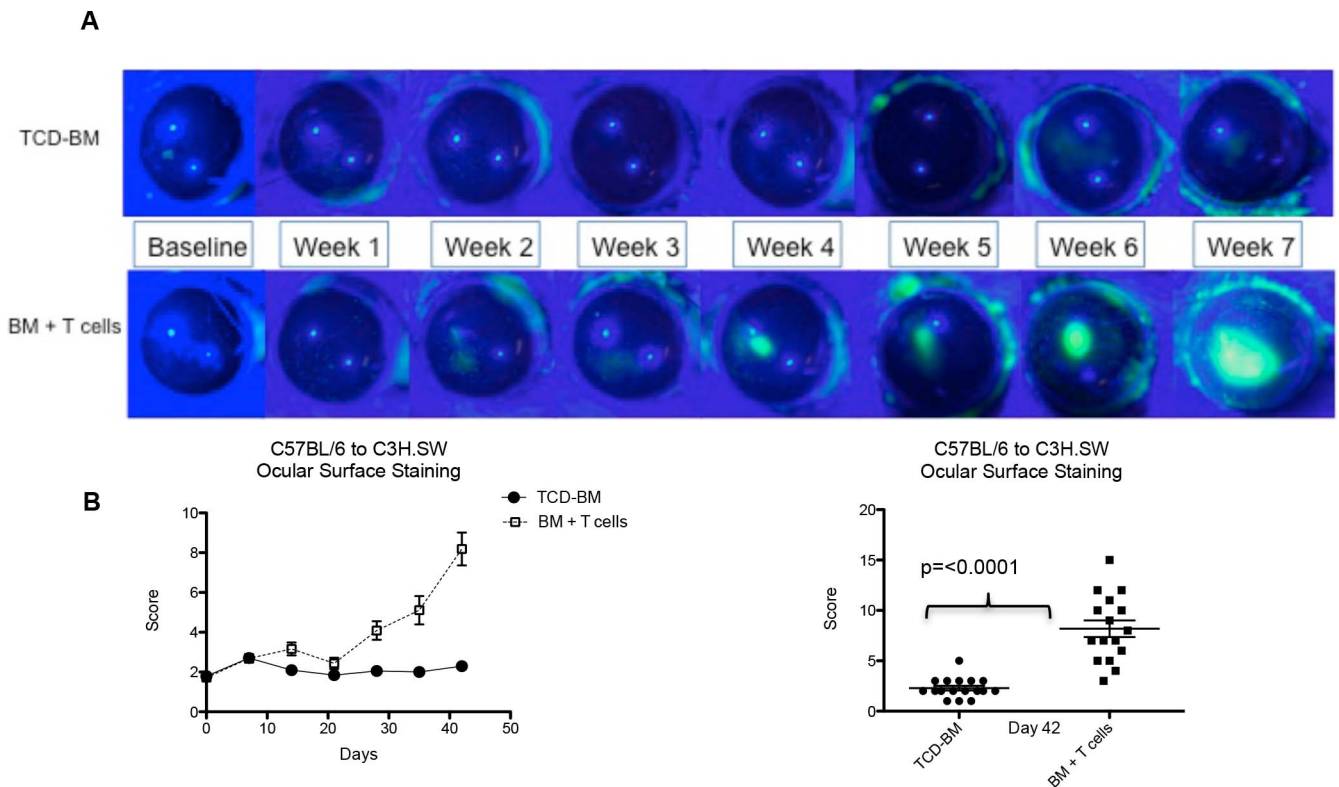


FIGURE 1. Systemic GVHD in C3H.SW recipients post HSCT. (A) Mice that received T cells developed high systemic GVHD scoring. Photos representative of mice without (B) and with (C) GVHD characterized by weight loss, ruffled fur, and poor posture. Systemic GVHD was confirmed by low number of splenocytes (D) and B cells (E) in animals that received TCD-BM + T cells.



**FIGURE 2.** Ocular surface assessment post HSCT: clinical changes in the corneas of HSCT recipients. **(A)** Clinical photos through 7 weeks demonstrating progression of corneal staining and development of ulcers in the group that received transplantation with TCD-BM + T cells. **(B)** Quantification of corneal fluorescein staining throughout the study and at day 42 after transplantation.

**Quantitative RT/PCR**

Total RNA was isolated from corneas using the RNeasy kit (Qiagen, Valencia, CA, USA); then cDNA was generated with the Maxima First Strand cDNA Synthesis Kit (Fermentas, Thermo Fisher, Grand Island, NY, USA). Gene expression was measured by real-time quantitative PCR (qPCR) using various

primers (see below). Quantitative PCR was performed using iQ SYBR Green Supermix (Bio-Rad, Hercules, CA, USA) on a Roche Light Cycler real-time PCR instrument (Roche, Indianapolis, IN, USA). Relative gene expression was calculated using the  $\Delta\Delta C_t$  method, with gene expression normalized to glyceraldehyde 3-phosphate dehydrogenase (GAPDH) expres-

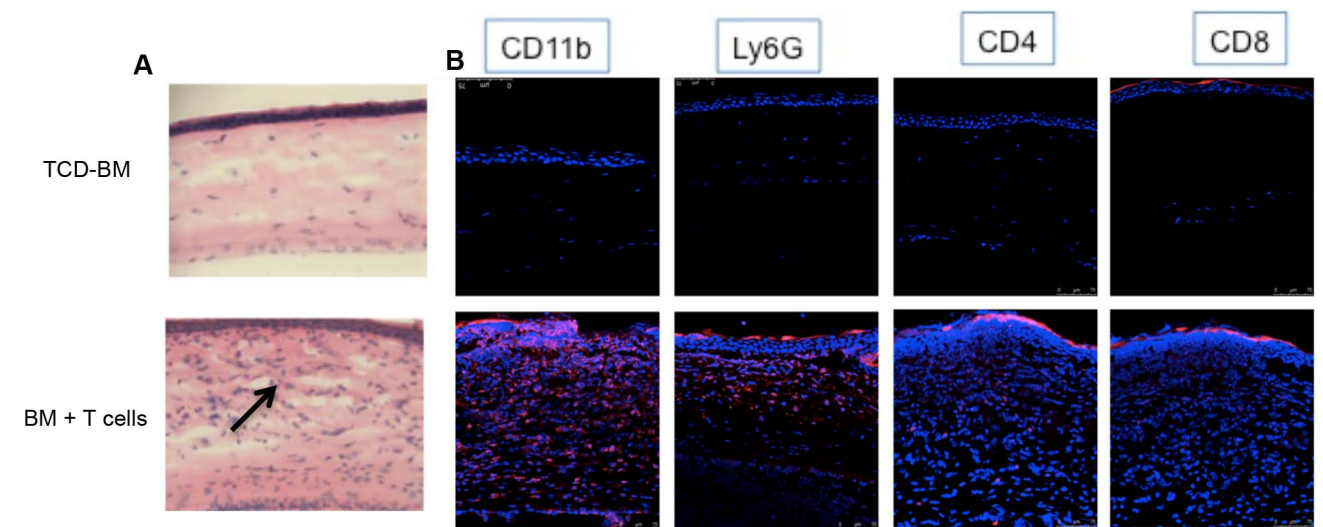


**FIGURE 3.** Pathologic changes in the corneas of allogeneic HSCT recipients. **(A)** Photographs (H&E stained, 7- $\mu$ m sections,  $\times 20$ ) of the central corneas of mice receiving B6 TCD-BM only or together with B6 T cells. Dense cellular infiltrates (*black arrow*) are observed in the eyes of animals with systemic GVHD. **(B)** Immunofluorescent microscopy. Photographs of 7- $\mu$ m sections at  $\times 40$  stained with CD11b (macrophages), Ly6G (neutrophils), CD4, CD8 (T cells), mAbs (*red*), and DAPI (*blue*). Cellular infiltrates in animals with GVHD consist of T cells, macrophages, and neutrophils.

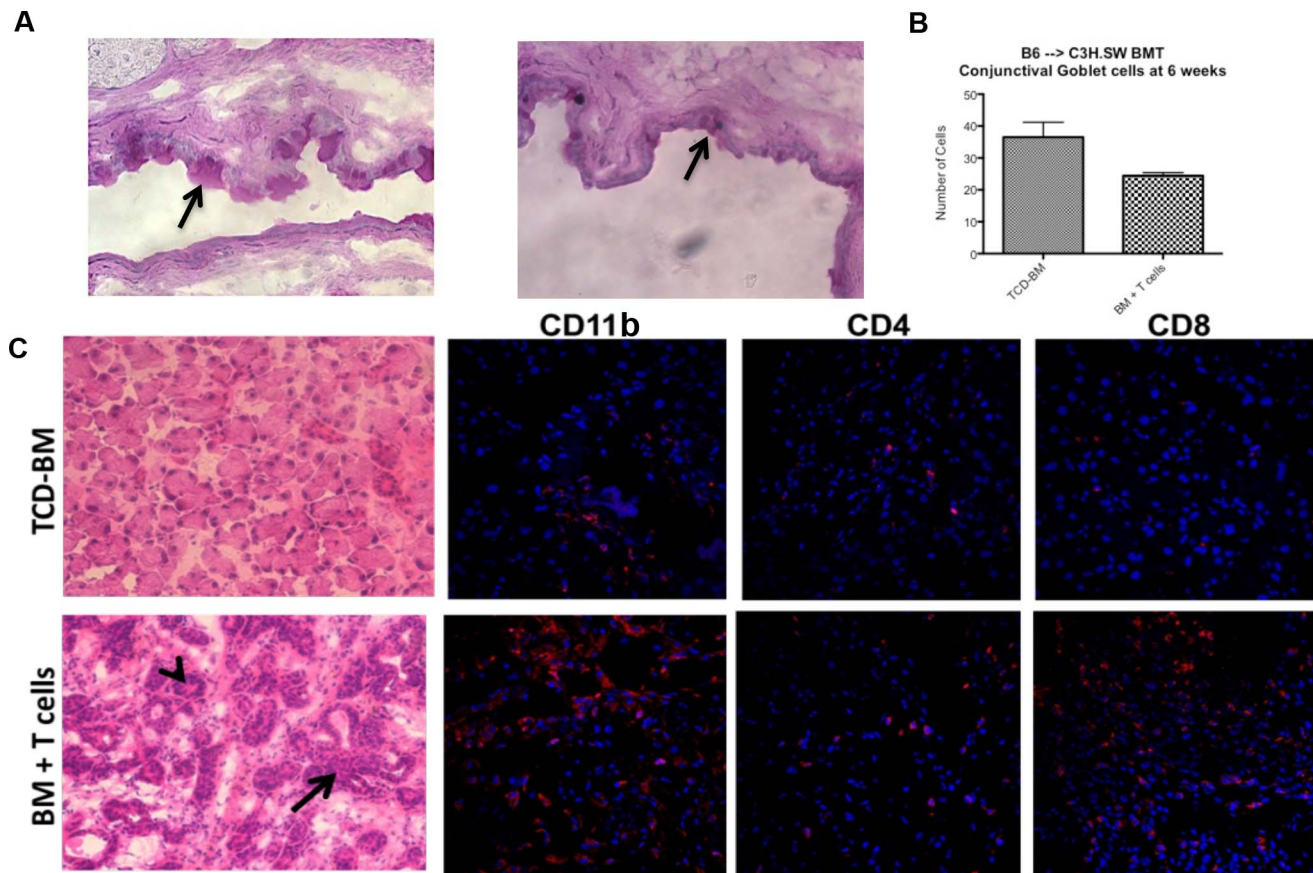


**FIGURE 4.** Involvement of the ocular adnexa in mice with GVHD. (A) Photographs (PAS-stained, 7- $\mu$ m sections,  $\times 20$ ) of the central superior conjunctiva of mice receiving B6 TCD-BM only or together with B6 T cells, where goblet cells stain *dark pink* (*black arrow*). Mice with GVHD exhibited thickening and irregularity of the basal membrane, as well as atrophy and reduced number of goblet cells (B). (C) Photographs of lacrimal gland histology from mice receiving TCD-BM only or together with T cells. Sections are 7  $\mu$ m thick and stained with H&E at  $\times 20$  magnification. Periductal fibrosis, dense cellular infiltrates (*black arrow*), and stasis of secretions in ducts (*arrowheads*) are observed in lacrimal glands of animals with systemic GVHD.

sion. Each treatment is represented as relative expression (i.e., fold expression over reference group), where the control sample served as the reference with a set value of 1. Primer pairs for cytokines were generated by IDT (Coralville, IA, USA).

GAPDH, Fwd: AGGTCGGTGTGAACGGATTTG,  
 Rev: TGTAGACCATGTAGTTGAGGTCA  
 IFN $\gamma$ , Fwd: ATGAACGCTACACTGCATC,  
 Rev: CCATCCTTTTGCCAGTTTCCTC  
 TNF $\alpha$ , Fwd: CTGAACTTCGGGGTGATCGG,  
 Rev: GGCTTGCTCACTCGAATTTTGAGA  
 IL6, Fwd: TAGTCCTTCCTACCCCAATTTCC,  
 Rev: TTGGTCTTAGCCACTCCTC

### Statistical Analysis

The unpaired *t*-test was used to compare between control and experimental for fluorescein staining and conjunctival goblet cell score. Both eyes were evaluated for ocular surface staining, and the eye with the worse fluorescein staining score was selected for statistical analysis (note that the data were also statistically significant including both eyes or using the least affected eye). A *P* value of 0.05 was considered statistically significant. GraphPad Prism 5 (GraphPad Software, San Diego, CA, USA) was used for the analyses.

## RESULTS

### Clinical Ocular Changes in Recipients Undergoing GVHD in an Major Histocompatibility Complex (MHC)-Matched, Minor Transplantation Antigen-Mismatched Allogeneic Hematopoietic Stem Cell Transplant Model

MHC-matched (H2<sup>b</sup>) C3H.SW mice were lethally conditioned and several hours later received donor B6 BMCs replete with B6 T cells (Table). Several weeks post HSCT, animals receiving donor T cells lost weight and began to exhibit clinical signs characteristic of GVHD including ruffled fur, hunching, and diarrhea (Figs. 1A–C). Recipients were examined for additional immunologic phenotypes characteristic of GVHD including decreased splenic cell numbers and diminished B cells (Figs. 1D, 1E). To monitor for changes in the ocular surface in recipients of HSCT, animals were anaesthetized and the corneal surface was assessed by clinical examination and fluorescein staining. Approximately 3 to 4 weeks following transplantation, increased fluorescein staining was observed only in the cornea of recipient mice that received donor T cells, and this progressed to corneal ulcerative lesions by  $\sim 6$  weeks (Fig. 2A). Quantitative analyses for corneal staining and clinical changes demonstrated a difference in the tempo of induction between systemic and ocular GVHD (Fig. 2B).

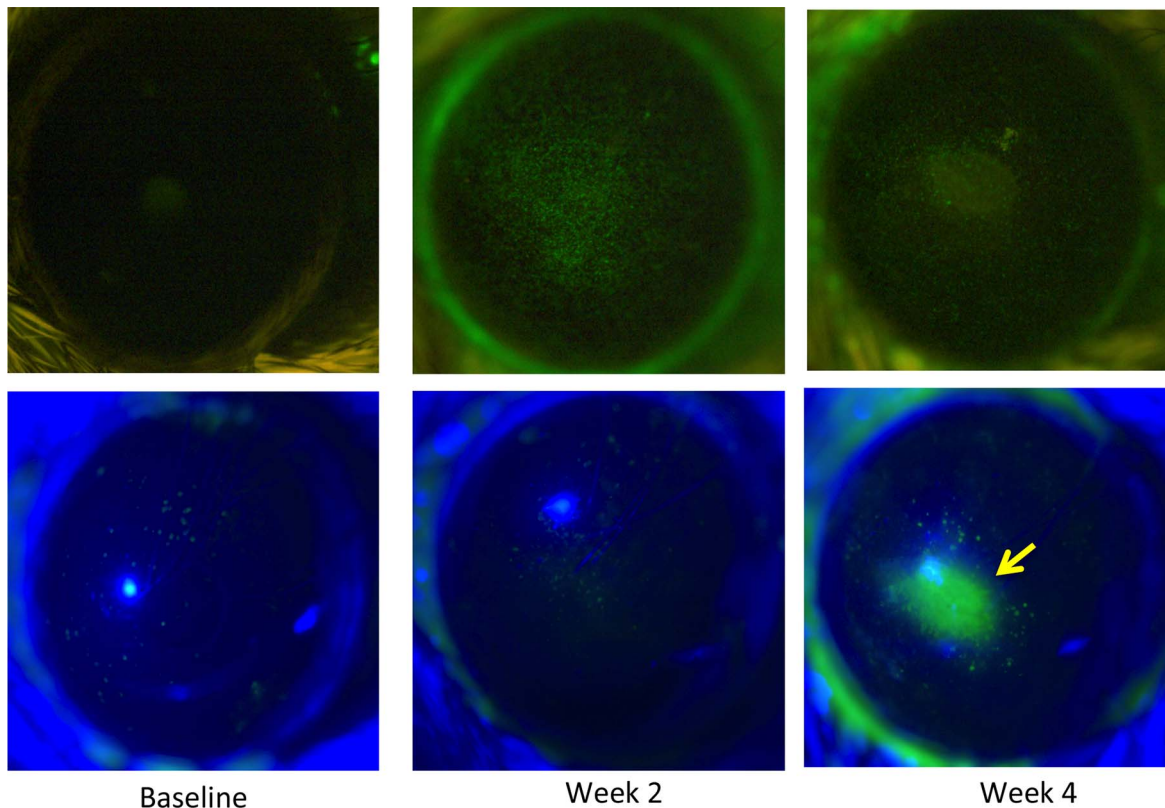


**FIGURE 5.** Identification of donor T-cell populations in recipient corneas of mice with GVHD. Mice received BM-TCD from B6-CD45.1 donors + T cells from B6-EGFP donors. *Top:* Donor EGFP<sup>+</sup> T cells were identified in vivo in the recipient corneas using fluorescent stereomicroscopy by 2 to 3 weeks post transplant (*top middle and right*). Clinical examination of the ocular surface (*bottom*) demonstrated the development of corneal ulcers approximately 4 to 6 weeks post transplant (*bottom right, arrow*). Data presented are from individual transplant recipient. T-cell infiltrates preceding clinical evidence of ocular surface disease were observed in seven mice in two independent experiments.

### Histopathologic Damage of the Ocular Surface and Adnexa of Animals With GVHD

To begin to characterize the damage occurring in the ocular compartment of animals with GVHD, the eyes were assessed for histopathologic changes and cellular infiltrates (Fig. 3). Histologic analyses demonstrated that only mice that developed systemic and ocular GVHD exhibited corneal thickening and epithelial irregularity, as well as dense inflammatory cell infiltrates (Fig. 3, left). Immunohistochemistry revealed that multiple mononuclear cells had infiltrated the cornea as evidenced by CD11b<sup>+</sup>-stained cells (which microscopically appeared to be macrophages) as well as CD4<sup>+</sup> and some CD8<sup>+</sup> T cells (Fig. 3). The presence of Ly6G-staining cells supports the notion that monocytes and neutrophils may also contribute to the observed infiltrate. Analyses of ocular adnexa indicated that the fornix region of the conjunctiva appeared atrophic and goblet cells were reduced in density and number (Figs. 4A, 4B). Hematoxylin/eosin- and Masson's trichrome-stained sections of the lacrimal glands revealed periductal fibrosis (red) and dense cellular infiltrates (black arrows), which consisted of predominantly macrophages (CD11b) and CD8<sup>+</sup> T cells together with some CD4<sup>+</sup> infiltrate (Fig. 4C, Supplementary Fig. S1). These data indicate that similar to ocular GVHD occurring in patients who undergo HSCT, all the structures of the ocular adnexa in this preclinical model of GVHD are involved and can lead to sicca and scarring.<sup>31,32</sup>

### Identification of Donor T-Cell Populations Infiltrating the Ocular Compartment in GVHD

Our findings above demonstrated the presence of immunologic cells recruited to the site of ocular inflammation. The presence of lymphoid cells in the ocular compartment could be the result of cells from three sources, that is, recipient, transplanted donor T cells, or transplanted donor stem cells that resulted in the production of de novo thymopoiesis. To determine if cells were of donor or recipient origin, transplants were performed using T cells derived from B6-EFGP mice (Table). Recipient C3H.SW mice of transplants containing T cells from B6-EGFP donors together with marrow cells from congenic, GFP<sup>-</sup> CD45.1 donors developed ulcerative lesions, and GFP<sup>+</sup> cells were clearly identified by intravital fluorescent microscopy of the eyes (Fig. 5). Notably, the appearance of T cells was first identified 2 to 3 weeks post transplant and prior to corneal ulceration (Fig. 5, upper).

To assess the relative T-cell subsets present, corneal lysates were prepared ~6 weeks post HSCT and cells stained for CD4 or CD8 expression (Fig. 6). The CD4/CD8 ratio is typically inverted in the periphery of these mice undergoing GVHD as evidenced in the spleen (Fig. 6) and other lymphoid tissue. However, the ratio of these T-cell subsets in the cornea and, interestingly, draining cervical nodes was not inverted, as evidenced by a slightly >1 ratio (Fig. 6).

To determine the precise origin, that is, bone marrow and/or transplanted T-cell source of the donor T cells, an experiment was performed using donor T cells from B6-

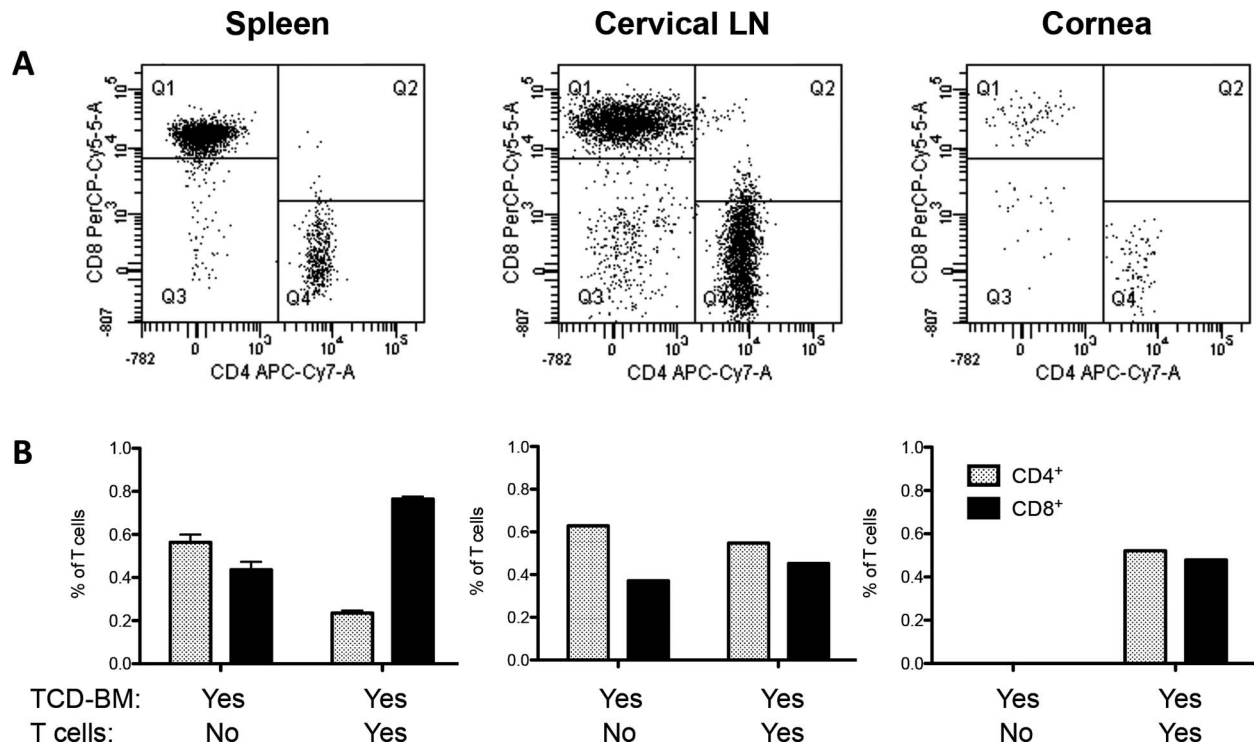


**FIGURE 6.** CD4/CD8 ratio differs dependent on the “target tissue.” Mice received BM-TCD from B6-CD45.1 donors + T cells from B6-EGFP donors. (A) Splens of mice that received TCD-BM + T cells displayed the characteristic GVHD phenotype, with increased number of CD8<sup>+</sup> T cells compared to CD4<sup>+</sup> cells, and a decreased CD4<sup>+</sup>/CD8<sup>+</sup> ratio. Data represent analysis of cells gated on EGFP<sup>+</sup> cells. *Quadrants* represent Q1, donor GFP<sup>+</sup>CD8<sup>+</sup> (PerCP-Cy5-5A); Q3, CD4<sup>+</sup>CD8<sup>-</sup>; Q4, donor GFP<sup>+</sup>CD4<sup>+</sup>(APC-Cy7-A). Interestingly, ocular compartments such as cornea and draining cervical lymph nodes showed equal or even higher amounts of CD4<sup>+</sup> cells compared to CD8<sup>+</sup> T cells, creating a higher CD4/8 ratio. (B) Spleen: Data represent three to five individual splens/group from one of two independent experiments. Cervical lymph nodes and cornea: Data represent pool of three to five mice/group from one of two independent experiments. Data are presented as fraction of total lymphocytes in each compartment.

CXCR6<sup>-/-EGFP</sup> knock-in mice (i.e., Bonzo/STRL33), which express EGFP regulated by the CXCR6 promoter (Table). Notably, high expression of EGFP was reportedly expressed on activated T-cell populations.<sup>33</sup> Importantly, C3H.SW recipients of B6-CXCR6<sup>-/-EGFP</sup> T cells lost weight and exhibited clinical changes of systemic GVHD (data not shown) and also developed ocular GVHD characterized by ulceration and infiltrate of the cornea (Figs. 7A–C). Moreover, ocular suspensions demonstrated the presence of GFP<sup>+</sup>Ly9.1<sup>-</sup> CD4 and CD8 T cells, confirming the presence of donor T cells in these recipients’ eyes (Figs. 7D, 7E). The relative CD4/CD8 ratio was as anticipated, slightly >1.0 (Fig. 7E). In summary, these results unequivocally demonstrate that transplanted donor T cells populate the ocular compartment in recipients with GVHD. Interestingly, the ocular infiltrate also contained cells in the GFP fraction (Fig. 7F) demonstrating the presence of CD4 and CD8 T cells (Fig. 7G). Also interestingly, these cells were Ly9.1<sup>-</sup> (Table) and therefore presumably derived from neither transplanted donor T cells (EGFP<sup>+</sup>) nor the recipient (Ly9.1<sup>+</sup>).

To begin to characterize the inflammatory milieu associated with the development of ocular GVHD, RNA was prepared from ocular lysates obtained from C3H.SW recipients of B6 T cell-depleted bone marrow alone or B6 T cell-replete transplants. The data illustrate that IFN $\gamma$ , TNF $\alpha$ , and IL-6 message were significantly elevated in mice with ocular GVHD (Fig. 8). In summary, the above findings illustrated that following allogeneic HSCT into MHC-matched allogeneic recipients, multiple populations of donor T cells are present in the ocular compartment that appear to be activated and derived from both donor-transplanted T cells and donor bone

marrow. Based on the use of the Bonzo/STRL33 donors, some infiltrating cells appear to be activated. We then employed donor T cells obtained from a B6-CD90.1 (Thy1.1<sup>+</sup>) congenic donor in an independent transplant experiment (Supplementary Fig. S1). The presence of Thy1.1<sup>+</sup> CD62L<sup>lo</sup> CD44<sup>hi</sup> CD4<sup>+</sup> T cells (as well as CD8<sup>+</sup>, data not shown) in the corneal lysates of these recipients confirmed that activated donor T cells were present in the ocular compartment.

## DISCUSSION

Ocular surface damage is a common occurrence in patients following allogeneic HSCT who develop GVHD.<sup>8,9,11–14</sup> Despite this life-altering complication, little is understood regarding the precise mechanisms underlying the immune-mediated pathogenesis. To understand the immune mechanisms responsible for the development of ocular GVHD, an MHC-matched minor histocompatibility-mismatched HSCT model that mimics matched unrelated donor (i.e., MUD) clinical transplants was developed in our laboratory.<sup>25,26</sup> Although no specific minor histocompatibility antigens (mHags) have been defined in the strain combination employed in the present studies, following allogeneic T cell-replete HSCT between MHC-matched donor/recipient pairs (e.g., B6/C3H.SW), mHags are known to induce GVHD.<sup>34</sup> C3H.SW-transplanted mice with B6 T cell-depleted bone marrow and T cells developed systemic GVHD ~3 weeks post HSCT as characterized by well-established immune phenotype (an inverted CD4/CD8 ratio and diminution of mature B cells). It is important to note that as a consequence of GVHD-induced damage to central lymphoid compartments, that is, the thymus

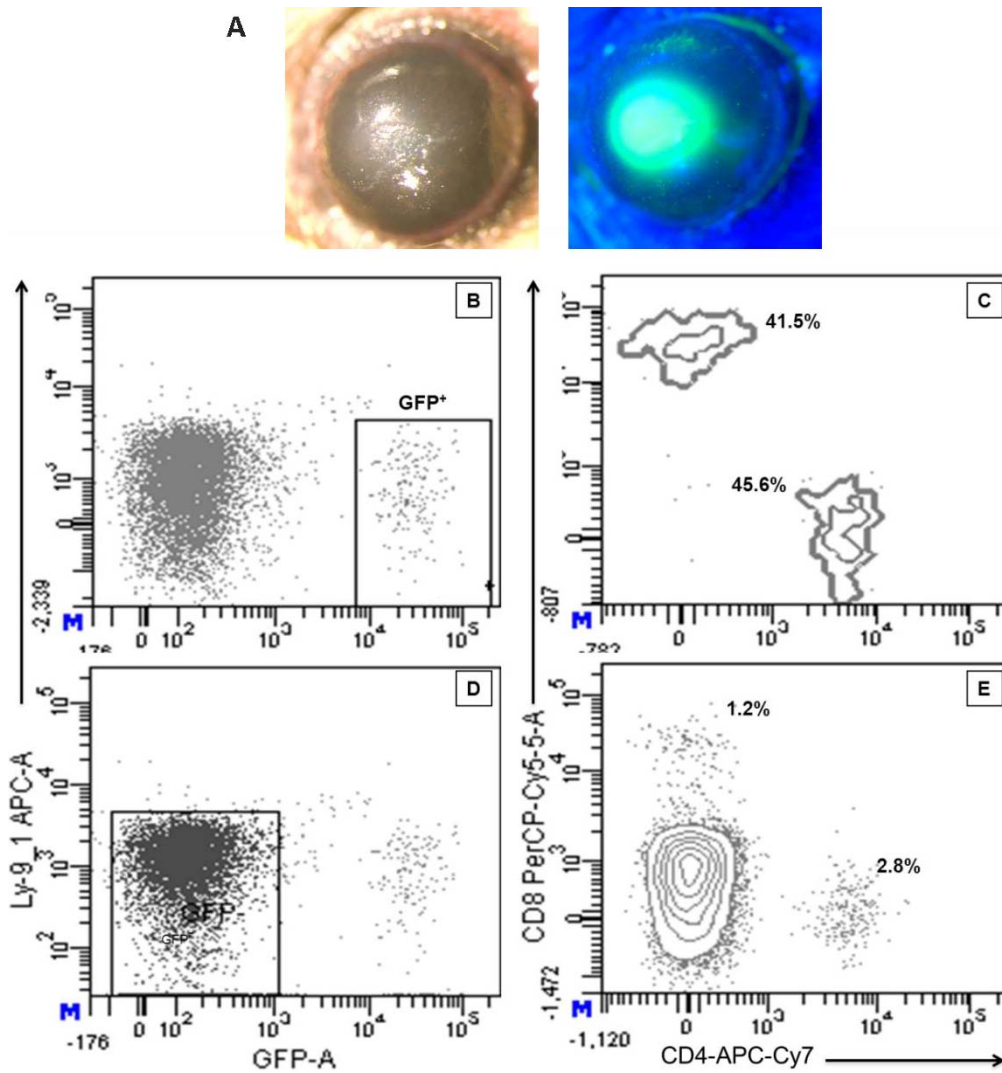


**FIGURE 7.** Subset analyses of T-cell infiltrate in the corneas of recipients with GVHD. Mice that received B6-CXCR6<sup>-/-</sup> EGFP developed clinical ocular changes characterized by ulceration (A). Flow cytometric analysis of corneal cell suspensions 5 weeks post transplant demonstrated the presence of a EGFP<sup>+</sup>Ly9.1<sup>-</sup> population (B), which contained both CD4 and CD8 lymphoid subsets (C), confirming the presence of donor T cells in the recipient corneas. The ocular infiltrate also contained GFP<sup>-</sup> cells (D) that could represent T cells (E) derived from either transplanted donor progenitor cells or the recipient. Results represent cells obtained from 10 pooled corneas (five transplant recipients).

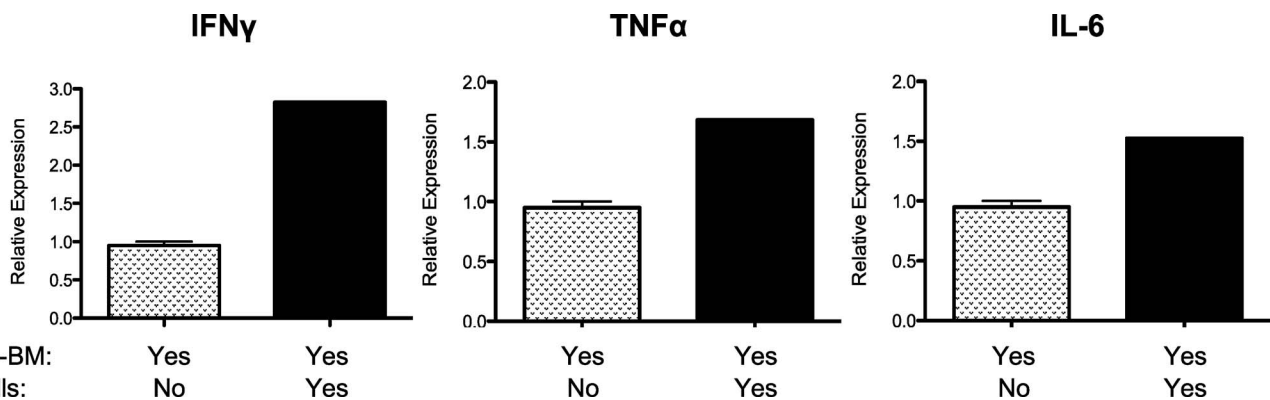


**FIGURE 8.** Inflammatory cytokines are elevated in the cornea of mice with ocular GVHD. RNA was prepared from corneal lysates obtained from C3H.SW recipients of B6 TCD-BM alone or B6 T cell-replete transplants (Table, line 1), and IL-6 mRNA was assessed by RT-PCR (see Methods). Results represent the mean of duplicate samples analyzed from pooled cornea extracts ( $n = 4$  corneas from two recipients) 4 to 5 weeks post transplant.



and bone marrow, mechanisms responsible for central tolerance are compromised, which may promote the generation of autoreactive donor T cells.<sup>20,35</sup> Importantly, these mice also developed ocular surface disease evidenced by progression of ocular surface damage characterized by increased corneal staining and ulceration by week 6. Within this context, it will be important to understand the underlying mechanism for ocular complications following allogeneic HSCT. Histologic analyses demonstrated that only mice that developed systemic and ocular GVHD exhibited corneal, lacrimal gland, and conjunctiva damage known to be a cause of sicca-mediated ocular injury. Although other ocular GVHD models have been reported to date, very few models mimic the clinical ocular manifestations occurring, and most are associated with acute models of the disease.<sup>23,24</sup> Moreover, the immune mechanisms involved in this process are poorly understood. We have developed a murine model of systemic and ocular GVHD after T cell-replete haematopoietic stem cell transplant (AHSCT), with onset kinetics similar to those observed in patients who develop eye complications following clinical AHSCT. In total, we conclude promising model that we have begun to utilize to dissect the underlying immune mechanisms leading to damage associated with ocular GVHD in allogeneic HSCT.

To determine the precise origin of the lymphocytic infiltrate detected in the ocular compartment, EGFP-labeled donor T cells were utilized, and monitoring by intravital microscopy documented their presence in the eye. Interestingly, the tempo of this recruitment occurred prior (~2–3 weeks) to ulceration, suggesting that these cells may contribute directly or indirectly to the pathologic findings observed. Notably, cellular infiltrates also contained a population of Ly9.1<sup>+</sup>/EGFP<sup>-</sup> (Table) cells derived from the donor bone marrow, and further analysis by immunohistochemistry identified a large number of CD11b<sup>+</sup> macrophages (Fig. 3), both of which could contribute to the damage occurring to the ocular surface. T cell-macrophage interactions could contribute to damage in other target tissues in GVHD.<sup>36</sup> We speculate that these are inflammatory macrophages, which may be the mediators of tissue damage including fibrosis in the ocular adnexa. Thus the interaction between T cell and macrophage populations is likely critical to this process and may represent novel targets for intervention for therapy. This is the initial report demonstrating the presence of donor T cells and macrophages in the ocular compartment, and therefore it will be important to determine if the infiltration of the latter is regulated by T cells. One explanation for the ocular pathology observed is that macrophages mediate damage, and we observed both inflammatory and effector cytokines including IL-6, TNF $\alpha$ , and IFN $\gamma$  lysates from affected eyes.

In the present study at the time points examined, we observed that the ocular infiltrating T cells are primarily from the donor inoculum. It may be notable that we also identified T cells apparently derived from donor stem cells. In any case, an interesting observation concerned the T-cell phenotype in the cornea and draining cervical lymph nodes (Fig. 3). In contrast to systemic CD4/CD8 ratios, in which CD4 > CD8, T cell infiltrates into the cornea and draining lymph nodes did not reflect this subset relationship in that there was a distinctly higher proportion of CD4<sup>+</sup> T cells. In this context it may be notable that we performed transplants using only CD4<sup>+</sup> donor T cells, and similar results systemically and locally were observed (Perez VL and Levy RB, unpublished observations, 2014). To further characterize the donor T-cell infiltrate we exploited the use of CXCR6-EGFP knock-in mice (i.e., Bonzo/STRL33).

These mice express EGFP regulated by the CXCR6 promoter, and notably high EGFP levels are preferentially expressed on activated and memory T cells.<sup>33</sup> The mice

employed in the present studies were homozygous and have been reported by other groups to mediate reduced hepatic GVHD.<sup>37</sup> Despite this deficiency, in the mHag-mismatched model used here, GVHD was induced as indicated in Figure 7A. We have also employed these mice to characterize T-cell recruitment into the eye during corneal allograft rejection and identified the presence of activated T cells.<sup>38</sup> Similarly in this model of GVHD, we found CXCR6-EGFP donor T cells consistent with a role for these lymphocytes in induction of ocular GVHD, an observation confirmed using an independent (CD90.1<sup>+</sup>CD44<sup>hi</sup>CD62L<sup>lo</sup>) donor. Interestingly, the identification of these T cells supports the notion of the local presence of activated T cells with a TH1 effector phenotype (i.e., IFN $\gamma$  and TNF $\alpha$ ) consistent with an antihost alloreactive population. In fact, this profile is similar to that observed in tear fluid of patients undergoing ocular GVHD.<sup>39</sup> These T cells may be directly and/or indirectly involved with tissue damage and in orchestrating the recruitment and activation of pathogenic macrophages.<sup>36</sup>

The primary objective of the present study was to identify the kinetics and origin of ocular infiltrating T cells in a preclinical model of GVHD inducing eye tissue injury.<sup>21</sup> Overall, the findings here demonstrated that mature T cells from the transplanted donor population, as well as some originating from the transplanted marrow, reached the ocular compartment in animals undergoing GVHD. In total, the results describe a novel and promising preclinical model characterized by both systemic and ocular changes following allo-HSCT, which will facilitate dissecting the underlying immune mechanisms leading to damage associated with ocular GVHD. Because most allo-HSCT are performed in patients with leukemia and lymphoma, the present model should help in development of locally administered therapies to regulate ocular complications while minimizing global immunosuppression permitting graft versus leukemia (GVL) responses.

### Acknowledgments

The authors thank Astrid Gonzalez and Ying Wang for their technical expertise and Jose Echeagaray for his help in animal maintenance. We also thank the Flow Cytometry Facilities of the Diabetes Research Institute (Oliver Umland) and Sylvester Cancer Center (Shannon Opiela and Patricia Guevara) for their help and support.

Supported by National Institutes of Health (NIH) National Eye Institute Grant R01 EY024484-01 (VLP, RBL) and NIH P30EY014801, unrestricted grant from Research to Prevent Blindness, and Walter G. Ross Ophthalmic Research (VLP).

Disclosure: **S. Herretes**, None; **D.B. Ross**, None; **S. Duffort**, None; **H. Barreras**, None; **T. Yaohong**, None; **A.M. Saeed**, None; **J.C. Murillo**, None; **K.V. Komanduri**, None; **R.B. Levy**, Allergan (C); **V.L. Perez**, Allergan (C)

### References

- Li HW, Sykes M. Emerging concepts in haematopoietic cell transplantation. *Nat Rev Immunol*. 2012;12:403–416.
- Martin PJ, Inamoto Y, Carpenter PA, Lee SJ, Flowers MED. Treatment of chronic graft-versus-host disease: past, present and future. *Korean J Hematol*. 2011;46:153–163.
- Arora M, Klein JP, Weisdorf DJ, Hassebroek A, Flowers ME, Cutler CS, et al. Chronic GVHD risk score: a Center for International Blood and Marrow Transplant Research analysis. *Blood*. 2011;117:6714–6720.
- Blazar BR, Murphy WJ, Abedi M. Advances in graft-versus-host disease biology and therapy. *Nat Rev Immunol*. 2012;12:443–458.

5. Ferrara JL, Levine JE, Reddy P, Holler E. Graft-versus-host disease. *Lancet*. 2009;373:1550-1561.
6. Filipovich AH, Weisdorf D, Pavletic S, Socie G, Wingard JR, Lee SJ, et al. National Institutes of Health consensus development project on criteria for clinical trials in chronic graft-versus-host disease: I. Diagnosis and staging working group report. *Biol Blood Marrow Transplant*. 2005;11:945-956.
7. Vigorito AC, Weisdorf D, Pavletic S, Socie G, Wingard JR, Lee SJ, et al. Evaluation of NIH consensus criteria for classification of late acute and chronic GVHD. *Blood*. 2009;114:702-708.
8. Franklin RM, Kenyon KR, Tutschka PJ, Saral R, Green WR, Santos GW. Ocular manifestations of graft-vs-host disease. *Ophthalmology*. 1983;90:4-13.
9. Hirst LW, Jabs DA, Tutschka PJ, Green WR, Santos GW. The eye in bone marrow transplantation. I. Clinical study. *Arch Ophthalmol*. 1983;101:580-584.
10. Inagaki E, Ogawa Y, Matsumoto Y, Kawakita T, Shimmura S, Tsubota K. Four cases of corneal perforation in patients with chronic graft-versus-host disease. *Mol Vis*. 2011;17:598-606.
11. Riemens A, te Boome L, Imhof S, Kuball J, Rothova A. Current insights into ocular graft-versus-host disease. *Curr Opin Ophthalmol*. 2010;21:485-494.
12. Tabbara KF, Al-Ghamdi A, Al-Mohareb F, Ayas M, Chaudhri N, Al-Sharif F, et al. Ocular findings after allogeneic hematopoietic stem cell transplantation. *Ophthalmology*. 2009;116:1624-1629.
13. Hessen M, Akpek EK. Ocular graft-versus-host disease. *Curr Opin Allergy Clin Immunol*. 2012;12:540-547.
14. Kim SK. Update on ocular graft versus host disease. *Curr Opin Ophthalmol*. 2006;17:344-348.
15. Clave E, Rocha V, Talvensaar K, Busson M, Douay C, Appert ML, et al. Prognostic value of pretransplantation host thymic function in HLA-identical sibling hematopoietic stem cell transplantation. *Blood*. 2005;105:2608-2613.
16. Fukushi N, Arase H, Wang B, Ogasawara K, Gotohda T, Good RA, et al. Thymus: a direct target tissue in graft-versus-host reaction after allogeneic bone marrow transplantation that results in abrogation of induction of self-tolerance. *Proc Natl Acad Sci U S A*. 1990;87:6301-6305.
17. Ghayur T, Seemayer TA, Xenocostas A, Lapp WS. Complete sequential regeneration of graft-vs.-host-induced severely dysplastic thymuses. Implications for the pathogenesis of chronic graft-vs.-host disease. *Am J Pathol*. 1988;133:39-46.
18. Parkman R. Graft-versus-host disease: an alternative hypothesis. *Immunol Today*. 1989;10:362-364.
19. Weinberg K, Blazar BR, Wagner JE, Agura E, Hill BJ, Smogorzewska M, et al. Factors affecting thymic function after allogeneic hematopoietic stem cell transplantation. *Blood*. 2001;97:1458-1466.
20. Rangarajan H, Yassai M, Subramanian H, Komorowski R, Whitaker M, Gorski J, et al. Emergence of T cells that recognize nonpolymorphic antigens during graft-versus-host disease. *Blood*. 2012;119:6354-6364.
21. Reddy P, Negrin R, Hill GR. Mouse models of bone marrow transplantation. *Biol Blood Marrow Transplant*. 2008;14(1 suppl 1):129-135.
22. Schroeder MA, DiPersio JF. Mouse models of graft-versus-host disease: advances and limitations. *Dis Model Mech*. 2011;4:318-333.
23. Hassan AS, Clouthier SG, Ferrara JL, Stepan A, Mian SI, Ahmad AZ, et al. Lacrimal gland involvement in graft-versus-host disease: a murine model. *Invest Ophthalmol Vis Sci*. 2005;46:2692-2697.
24. Perez RL, Pérez-Simón JA, Caballero-Velazquez T, Flores T, Carrancio S, Herrero C, et al. Limbus damage in ocular graft-versus-host disease. *Biol Blood Marrow Transplant*. 2011;17:270-273.
25. Baker MB, Altman NH, Podack ER, Levy RB. The role of cell-mediated cytotoxicity in acute GVHD after MHC-matched allogeneic bone marrow transplantation in mice. *J Exp Med*. 1996;183:2645-2656.
26. Baker MB, Riley RL, Podack ER, Levy RB. Graft-versus-host-disease-associated lymphoid hypoplasia and B cell dysfunction is dependent upon donor T cell-mediated Fas-ligand function, but not perforin function. *Proc Natl Acad Sci U S A*. 1997;94:1366-1371.
27. Cooke KR, Kobzik L, Martin TR, Brewer J, Delmonte J Jr, Crawford JM, et al. An experimental model of idiopathic pneumonia syndrome after bone marrow transplantation: I. The roles of minor H antigens and endotoxin. *Blood*. 1996;88:3230-3239.
28. Bron AJ, Evans VE, Smith JA. Grading of corneal and conjunctival staining in the context of other dry eye tests. *Cornea*. 2003;22:640-650.
29. Lemp MA. Report of the National Eye Institute/Industry workshop on Clinical Trials in Dry Eyes. *CLAO J*. 1995;21:221-232.
30. Carlson EC, Drazba J, Yang X, Perez VL. Visualization and characterization of inflammatory cell recruitment and migration through the corneal stroma in endotoxin-induced keratitis. *Invest Ophthalmol Vis Sci*. 2006;47:241-248.
31. Dursun D, Wang M, Monroy D, Li DQ, Lokeshwar BL, Stern ME, et al. A mouse model of keratoconjunctivitis sicca. *Invest Ophthalmol Vis Sci*. 2002;43:632-638.
32. Suwan-apichon O, Rizen M, Rangsin R, Herretes S, Reyes JM, Lekhanont K, et al. Botulinum toxin B-induced mouse model of keratoconjunctivitis sicca. *Invest Ophthalmol Vis Sci*. 2006;47:133-139.
33. Unutmaz D, Xiang W, Sunshine MJ, Campbell J, Butcher E, Littman DR. The primate lentiviral receptor Bonzo/STRL33 is coordinately regulated with CCR5 and its expression pattern is conserved between human and mouse. *J Immunol*. 2000;165:3284-3292.
34. Korngold R, Sprent J. Variable capacity of L3T4+ T cells to cause lethal graft-versus-host disease across minor histocompatibility barriers in mice. *J Exp Med*. 1987;165:1552-1564.
35. Hollander GA, Widmer B, Burakoff SJ. Loss of normal thymic repertoire selection and persistence of autoreactive T cells in graft vs host disease. *J Immunol*. 1994;152:1609-1617.
36. Murray PJ, Wynn TA. Protective and pathogenic functions of macrophage subsets. *Nat Rev Immunol*. 2011;11:723-737.
37. Sato T, Thorlacijs H, Johnston B, Staton TL, Xiang W, Littman DR, et al. Role for CXCR6 in recruitment of activated CD8+ lymphocytes to inflamed liver. *J Immunol*. 2005;174:277-283.
38. Tan Y, Abdulreda MH, Cruz-Guilloty F, Cutrufello N, Shishido A, Martinez RE, et al. Role of T cell recruitment and chemokine-regulated intra-graft T cell motility patterns in corneal allograft rejection. *Am J Transplant*. 2013;13:1461-1473.
39. Riemens A, Stoyanova E, Rothova A, Kuiper J. Cytokines in tear fluid of patients with ocular graft-versus-host disease after allogeneic stem cell transplantation. *Mol Vis*. 2012;18:797-802.